LIMNOLOGY and OCEANOGRAPHY

ASLO

Limnol. Oceanogr. 60, 2015, 2145–2157

doi: 10.1002/lno.10161

The modulating effect of light intensity on the response of the coccolithophore *Gephyrocapsa oceanica* to ocean acidification

Yong Zhang,*[1] Lennart T. Bach,[1] Kai G. Schulz,[2] Ulf Riebesell[1]

[1]Biological Oceanography, GEOMAR Helmholtz-Centre for Ocean Research Kiel, Kiel, Germany

[2]Centre for Coastal Biogeochemistry, School of Environmental Science and Management, Southern Cross University, Lismore, New South Wales, Australia

Abstract

Global change leads to a multitude of simultaneous modifications in the marine realm among which shoaling of the upper mixed layer, leading to enhanced surface layer light intensities, as well as increased carbon dioxide (CO_2) concentration are some of the most critical environmental alterations for phytoplankton. In this study, we investigated the responses of growth, photosynthetic carbon fixation and calcification of the coccolithophore *Gephyrocapsa oceanica* to elevated P_{CO_2} (51 Pa, 105 Pa, and 152 Pa) (1 Pa ≈ 10 μatm) at a variety of light intensities (50–800 μmol photons m^{-2} s^{-1}). By fitting the light response curve, our results showed that rising P_{CO_2} reduced the maximum rates for growth, photosynthetic carbon fixation and calcification. Increasing light intensity enhanced the sensitivity of these rate responses to P_{CO_2}, and shifted the P_{CO_2} optima toward lower levels. Combining the results of this and a previous study (Sett et al. 2014) on the same strain indicates that both limiting low P_{CO_2} and inhibiting high P_{CO_2} levels (this study) induce similar responses, reducing growth, carbon fixation and calcification rates of *G. oceanica*. At limiting low light intensities the P_{CO_2} optima for maximum growth, carbon fixation and calcification are shifted toward higher levels. Interacting effects of simultaneously occurring environmental changes, such as increasing light intensity and ocean acidification, need to be considered when trying to assess metabolic rates of marine phytoplankton under future ocean scenarios.

Atmospheric carbon dioxide (CO_2) concentrations are projected to increase from about 40 Pa (1 Pa ≈ 10 μatm) in 2013 beyond 75 Pa by the end of this century (IPCC 2013). Until today about one third of all anthropogenic CO_2 emissions have been absorbed by the ocean (Sabine et al. 2004). Increasing seawater CO_2 forms carbonic acid leading to a reduction in seawater pH. The pH of oceanic surface seawater is projected to decrease by 0.3–0.4 units within the next 100 yr (Houghton et al. 2001), representing a 100–150% increase in the proton concentration ($[H^+]$). These changes in CO_2 and $[H^+]$ can have positive effects for some phytoplankton functional groups while effects can be negative for others (Riebesell 2004).

Global warming, associated with increasing atmospheric CO_2 levels, enhances vertical stratification of the water column and decreases mixing between the surface ocean and deeper layers (Bopp et al. 2001). This expected shoaling of the upper mixed layer increases the average light intensity experienced by phytoplankton suspended in this layer (Sarmiento et al. 2004). Elevated light intensity may accelerate growth rates of some phytoplankton groups, while it might be stressful to others (Merico et al. 2004). When solar irradiance exceeds the capacity of common protective mechanisms, growth and electron transport rates of phytoplankton can be reduced (Gao et al. 2012). Depending on their photosynthetic apparatus, phytoplankton differ in their ability to cope with excess light intensities (Kaeriyama et al. 2011).

Most microalgae have developed energetically costly CO_2-concentrating mechanisms (CCMs) to avoid inorganic carbon limitation at the site of fixation (Giordano et al. 2005). CCMs involve the active uptake of CO_2 and/or HCO_3^- into the algal cell and/or the chloroplast. Given that the operation of CCMs is energetically costly, light availability may affect the activity of CCMs and the activity of CCMs may affect the energy reallocation in phytoplankton (Giordano et al. 2005). Energy saved from the down-regulation of CCMs in response to elevated CO_2 permits utilization in other processes such as growth or enzyme synthesis (Schippers et al. 2004; McCarthy et al. 2012).

Coccolithophores play an important role in the marine carbon cycle through the fixation of inorganic carbon via photosynthesis, as well as the precipitation of calcium

*Correspondence: yzhang@geomar.de

carbonate (Rost and Riebesell 2004). Coccolith formation has been suggested to reduce the risk of photo-damage of coccolithophores under high light conditions either by shading the cells like a sunshade (Braarud et al. 1952) or by contributing to excess energy dissipation (Barcelos e Ramos et al. 2012; Xu and Gao 2012). Declining pH generally reduces calcification rates (Bach et al. 2011; Riebesell and Tortell 2011), which may then put the cells at higher risk to suffer from photo-inhibition.

In this study, we investigated the combined effects of three P_{CO_2} levels and six light intensities on the cosmopolitan coccolithophore *Gephyrocapsa oceanica*. We measured the relative electron transport rate (rETR), growth rate, as well as carbon fixation and calcification rates to assess how light intensity modulates the effect of increasing P_{CO_2} on these parameters in *G. oceanica*.

Methods

Experimental setup

Gephyrocapsa oceanica (strain RCC 1303, isolated from Arcachon Bay, France in 1999) was grown in artificial seawater (ASW) under dilute batch culture conditions at 20°C. Light intensities were set to 50 μmol photons m^{-2} s^{-1}, 100 μmol photons m^{-2} s^{-1}, 200 μmol photons m^{-2} s^{-1}, 400 μmol photons m^{-2} s^{-1}, 600 μmol photons m^{-2} s^{-1}, and 800 μmol photons m^{-2} s^{-1} of photosynthetically active radiation (PAR) in a RUMED Light Thermostat (Rubarth Apparate GmbH) at a 16 : 8 h light : dark cycle. Light intensities were measured at every position in the light chamber where the bottles were put, using a Li-250A data logger (Li-Cor, Heinz Walz GmbH, Effeltrich).

ASW with a salinity of 35 was prepared according to Kester et al. (1967), but with the addition of 2350 μmol kg^{-1} bicarbonate (as opposed to 2330 μmol kg^{-1} in the original recipe). ASW was enriched with 64 μmol kg^{-1} nitrate (NO_3^-), 4 μmol kg^{-1} phosphate (PO_4^{3-}), f/8 concentrations for trace metals and vitamins (Guillard and Ryther 1962), 10 nmol kg^{-1} SeO_2 (Danbara and Shiraiwa 1999), and 2 mL kg^{-1} of sterile filtered (0.2 μm pore size, Sartobran® P 300, Sartorius) North Sea water to prevent possible trace metal limitation during culturing. Enriched ASW was aerated for 48 h at 20°C (0.2 μm pore size, Midisart® 2000 PTFE, Sartorius) with air containing 40, 84 or 112 Pa P_{CO_2} (ALPHAGAZ™). The dry air/CO_2 mixture was humidified with Milli-Q water before aeration into the ASW to minimize evaporation. After aeration, the ASW medium was sterile-filtered (0.2 μm pore size, Sartobran® P 300, Sartorius) with gentle pressure and carefully pumped into autoclaved 0.5 L or 2 L polycarbonate bottles (Nalgene® Bottles). Samples to assess carbonate chemistry conditions at the beginning of the experiment (total alkalinity (TA) and dissolved inorganic carbon (DIC) analysis) were taken from the sterile-filtered medium. 0.5 L bottles were used to acclimate cells to experimental conditions for 7–9 generations (one replicate, maximum final cell number in these acclimation cultures were 23,000 cells mL^{-1}). Depending on growth rate, acclimation time was between 9 (slowest growth) and 4 (fastest growth) days. The main experiment culture was conducted in 2 L bottles (four replicates). The initial cell concentrations in the main experiment culture and in the pre-culture were about 220 cells mL^{-1}. Bottles for both the acclimation culture and the main experiment were filled with ASW medium leaving a minimum headspace of less than 1% to keep gas exchange at a minimum. Cells were transferred from 0.5 L to 2 L bottles at the same time. The volume of the inoculum was calculated (*see* below) and the same volume of ASW was taken out from 2 L bottles before inoculation. All culture bottles were stored at the experimental temperature of 20°C for 3 or 4 d prior to inoculation. Culture bottles were manually rotated twice a day at 5 h and 12 h after the onset of the light phase to reduce sedimentation of the cells.

Carbonate chemistry measurements

Samplings started 3 h after the onset of the light period and lasted no longer than 2 h. Dissolved inorganic carbon (DIC) samples were sterile filtered (0.2 μm pore size, Filtropur S 0.2, Sarstedt) by gentle pressure into 50 mL Duran Winkler flasks (Schott). The bottles were filled with samples from bottom to top and with overflow, tightly closed without headspace, and stored at 4°C. DIC concentrations were measured by an infrared CO_2 analyzer system (Automated Infra Red Inorganic Carbon Analyzer, Marianda). Samples for total alkalinity (TA) measurements were filtered with GF/F filters (0.7 μm nominal pore size, Whatman), poisoned with a saturated $HgCl_2$ solution (0.5‰ final concentration), and stored at 4°C. TA was measured in duplicate by open-cell potentiometric titration using a 862 Compact Titrosample (Metrohm) according to Dickson et al. (2003). DIC and TA samples were collected and measured before and at the end of incubations. Measurements of DIC and TA were corrected with certified reference material (Batch 115, Prof. A. Dickson, La Jolla, California). The carbonate system was calculated from TA, DIC, phosphate, temperature, and salinity using the CO2 System Calculations in MS Excel software (Pierrot et al. 2006) with temperature and salinity dependent stoichiometric equilibrium constants K_1 and K_2 for carbonic acid taken from Roy et al. (1993).

Photosynthetic measurements

The effective quantum yield of photosystem II (PSII) of algae samples was assessed using a Phytoplankton Analyzer PHYTO-PAM (Heinz Walz GmbH) 5 h after the onset of the light phase. Samples were kept in the dark for 15 min at room temperature (about 20°C). Gain setting was adjusted with algae sample via the Auto-Gain function and the effect of background signal was suppressed with the help of the Zero Offset function with filtered culture water. PAR levels between 1 μmol photons m^{-2} s^{-1} and 1659 μmol photons

m^{-2} s^{-1} were applied in 14 steps of 30 s each in light response curve measurements.

The relative electron transport rate (rETR) was calculated according to Schreiber et al. (1995), where:

$$\text{rETR}=\text{Yield} \times \text{PAR} \times 0.5 \times 0.84 \ (\mu\text{mol electrons } m^{-2}s^{-1}) \quad (1)$$

where yield (F_v/F_m) is defined as the ratio of photons emitted to photons absorbed by PSII (Schreiber et al. 1995). Implicit in this equation is the assumption that half of the quanta of the incident PAR are distributed to PSII and 84% of incident PAR is absorbed by photosynthetic pigments in a standard leaf (Björkman and Demmig 1987).

Photosynthesis vs. irradiance curves (P-I curves) were obtained by plotting calculated rETR vs. corresponding PAR values. P-I curve fitting was performed using a theoretical light response function according to a modified version of the photosynthesis model of Eilers and Peeters (1988).

$$y=\frac{\text{PAR}}{a\times\text{PAR}^2+b\times\text{PAR}+c} \quad (2)$$

where the coefficients a, b and c are fitted in a least square manner. The model of Eilers and Peeters can be easily interpreted algebraically. At low light intensity, $b \times$ PAR and $a \times \text{PAR}^2$ can be neglected and y (ETR) increases approximately linearly with light intensity. At high light intensity, $a \times \text{PAR}^2$ dominates and thus y (ETR) is inversely proportional to the light intensity. The initial slope of the light limited part of the P-I curve constitutes a measure of the quantum yield of electron transport, indicated as alpha, which was calculated as:

$$\text{alpha}=\frac{1}{c} \quad (3)$$

The maximum value (Y_{max}) of rETR was calculated as:

$$Y_{max}=\frac{1}{b+2\sqrt{ac}} \quad (4)$$

Here, Y_{max} shows the saturation level of rETR (rETR_{max}). Saturation light intensity I_k corresponds to the PAR value at the crossing point of the lines defined by the initial slope and rETR_{max}. I_k is calculated from the expression rETR_{max}/alpha and is characteristic for the onset of light saturation.

Growth rate measurements

At the end of incubations, about 25 mL samples were taken from the culture bottles at the same time, ~ 7 h after the onset of the light phase. Cell numbers were determined using a Z2 Coulter Particle Counter and Size Analyzer (Beckman). Growth rate (μ) was calculated for each replicate according to the equation:

$$\mu=(\ln N_1-\ln N_0)/d \quad (5)$$

where N_0 and N_1 are cell numbers at the beginning and the end of a growth interval, and d is the duration of the growth period in days.

Particulate organic (POC) and inorganic carbon (PIC) measurements

Samples for total particulate carbon (TPC) and particulate organic carbon (POC) were gently filtered (200 mbar) onto pre-combusted (500°C, 8 h) GF/F filters and stored in the dark at −20°C. Prior to the measurement, POC filters were fumed with 37.1% HCl (w/w) for 2 h to remove all inorganic carbon. After 8 h of drying at 60°C, TPC and POC were measured using an isotope ratio mass spectrometer (Thermo Finnigan MAT 253 GmbH). Particulate inorganic carbon (PIC) was calculated as the difference between TPC and POC. POC and PIC production rates were calculated as:

$$\text{POC production rate}=\mu\left(d^{-1}\right)\times\text{POC content}\left(\text{pg C cell}^{-1}\right) \quad (6)$$

$$\text{PIC production rate }=\mu\left(d^{-1}\right)\times\text{PIC content }\left(\text{pg C cell}^{-1}\right) \quad (7)$$

Data analysis

Growth, POC and PIC production rates as a function of light intensity (PAR) were fitted at each P_{CO_2} level (51 Pa, 105 Pa, and 152 Pa) with the model of Eilers and Peeters (1988) (Eq. 2). The theoretical maximum rates for growth, POC and PIC production are calculated according to Eq. 4. Conversely, we fitted growth, POC and PIC production rates at each light intensity as a function of P_{CO_2} using the modified Michaelis–Menten equation:

$$y=\frac{X\times P_{CO_2}}{Y+P_{CO_2}}-s\times P_{CO_2} \quad (8)$$

derived by Bach et al. (2011). Here, s is the constant which describes the negative effect of increasing $[H^+]$ (which is quasi proportional to P_{CO_2} at constant TA). y is growth, POC or PIC production rate at a certain P_{CO_2} level. X and Y are random fit parameters which can be converted to the Michaelis–Menten parameters V_{max} and $K_{1/2}$ with a mathematical procedure described in Bach et al. (2011). The underlying assumption implicit in this equation is that growth, POC and PIC production rates follow an optimum curve over a broad range of P_{CO_2} values at constant TA, which has been shown for a variety of coccolithophore species (Langer et al. 2006; Bach et al. 2011; Sett et al. 2014; Bach et al. 2015).

The effect of the P_{CO_2} treatment on V_{max} was determined by means of a one-way analysis of variance (ANOVA). A two-way ANOVA was used to determine the main effect of P_{CO_2} and light treatments and their interactions for these

Table 1. Carbonate system parameters of the artificial seawater. DIC and TA samples were collected and measured before and at the end of incubations. The carbonate system parameters were calculated from TA, DIC, phosphate concentration (4 μmol kg^{-1}), temperature (20°C), and salinity (35) using the CO_2 System Calculations in MS Excel software (Pierrot et al. 2006).

P_{CO_2} Pa	TA μmol kg^{-1}	DIC μmol kg^{-1}	pH total scale	HCO_3^- μmol kg^{-1}	CO_3^{2-} μmol kg^{-1}	CO_2 μmol kg^{-1}	Ω calcite
51 ± 4^a	2294 ± 34^a	2066 ± 19^a	7.96 ± 0.04^a	1882 ± 17^a	167 ± 15^a	16.7 ± 1.6^a	4.0 ± 0.3^a
105 ± 9^b	2325 ± 14^b	2213 ± 19^a	7.69 ± 0.04^b	2080 ± 22^b	100 ± 8^b	34.1 ± 3.3^b	2.4 ± 0.2^b
152 ± 12^c	2331 ± 9.6^b	2196 ± 17^a	7.54 ± 0.03^c	2149 ± 17^c	74 ± 5^c	49.4 ± 4.4^c	1.8 ± 0.1^c

Characters a, b, c represent statistically different means between different P_{CO_2} treatments (Tukey Post hoc, $p < 0.001$). The values are expressed as mean values with standard deviation calculated from measurements before and at the end of incubations.

variables. A Tukey Post hoc test was performed to identify the source of the main effect determined by ANOVA. Normality of residuals was tested with a Shapiro–Wilk's test. Levene's test was conducted graphically to test for homogeneity of variances in case of significant data. A generalized least squares (GLS) model was used to stabilize heterogeneity if variances were inhomogeneous. All statistical calculations were performed using *R* version 2.15.2.

Results

Carbonate chemistry

All parameters (measured and calculated) of the carbonate system are presented in Table 1. Air pressure in the headspace of the 10 L bubbling bottles was about 25–35% higher than one standard atmosphere, leading to higher P_{CO_2} levels in air-saturated ASW than targeted P_{CO_2}. After aerating for 48 h at about 40, 84, and 112 Pa P_{CO_2}, the P_{CO_2} levels of the

Table 2. Results of two-way ANOVAs of the effects of P_{CO_2}, light intensity (PAR) and their interaction on μ, $rETR_{max}$, alpha, I_k, POC and PIC production rates, PIC : POC ratio, POC : PON ratio.

Parameter	Treatment	df	F value	*p* value
μ	P_{CO_2}	2	3928.30	<0.001
	PAR	5	18551.90	<0.001
	P_{CO_2}×PAR	10	1651.00	<0.001
$rETR_{max}$	P_{CO_2}	2	1544.10	=0.003
	PAR	5	1025.51	<0.001
	P_{CO_2}×PAR	10	25.89	<0.001
alpha	P_{CO_2}	2	21.80	<0.001
	PAR	5	644.00	<0.001
	P_{CO_2}×PAR	10	46.80	<0.001
I_k	P_{CO_2}	2	883.28	<0.001
	PAR	5	3312.69	<0.001
	P_{CO_2}×PAR	10	122.17	<0.001
POC production rate	P_{CO_2}	2	9174.71	<0.001
	PAR	5	3738.19	<0.001
	P_{CO_2}×PAR	10	55.36	<0.001
PIC production rate	P_{CO_2}	2	346.08	<0.001
	PAR	5	857.79	<0.001
	P_{CO_2}×PAR	10	107.97	<0.001
PIC : POC ratio	P_{CO_2}	2	627.001	<0.001
	PAR	5	28.994	<0.001
	P_{CO_2}×PAR	10	16.675	<0.001
POC : PON ratio	P_{CO_2}	2	20.46	<0.001
	PAR	5	19.85	<0.001
	P_{CO_2}×PAR	10	2.71	=0.009

PAR, photosynthetically active radiation (μmol photons m^{-2} s^{-1}); μ, growth rate (d^{-1}); $rETR_{max}$, maximum relative electron transport rate (μmol electrons m^{-2} s^{-1}); alpha, slope of the light-limited part of the photosynthesis versus irradiance curve; I_k, saturating photon flux density (μmol photons m^{-2} s^{-1}); POC production rate, particulate organic carbon production rate (pg C cell^{-1} d^{-1}); PIC production rate, particulate inorganic carbon production rate (pg C cell^{-1} d^{-1}).

ASW were about 51 Pa, 105 Pa, and 152 Pa, and resulting pH_T (reported on the total scale) were about 7.96, 7.69, and 7.54, respectively.

Growth rates

Light intensities and P_{CO_2} levels significantly affected growth rates in *G. oceanica*, both individually as well as interactively (Table 2). At a P_{CO_2} of 51 Pa, growth rates of *G. oceanica* increased with increasing light intensity until 800 μmol photons m^{-2} s^{-1}. At higher P_{CO_2} levels, however, growth rates only increased until 400 μmol photons m^{-2} s^{-1} and slightly declined thereafter (Fig. 1A).

At 50 μmol photons m^{-2} s^{-1}, growth rates of *G. oceanica* were similar at the three P_{CO_2} levels (Tukey Post hoc, $p > 0.1$). At 100 μmol photons m^{-2} s^{-1}, growth rate at 105 Pa P_{CO_2} was higher than at 51 and 152 Pa P_{CO_2} (Tukey Post hoc, $p < 0.001$) (Fig. 1; Table 3). At 200 μmol photons m^{-2} s^{-1} and above, growth rates decreased with elevated P_{CO_2} levels (Tukey Post hoc, all df = 2, all $p < 0.001$) (Fig. 1; Table 3). Fitted maximum growth rates declined significantly with rising P_{CO_2} levels (one-way ANOVA, $F = 3836$, df = 2, $p < 0.001$; Tukey Post hoc, df = 2, $p < 0.001$) (Fig. 1A; Table 4).

$rETR_{max}$, alpha and I_k

We identified statistically significant effects of light intensity, P_{CO_2} level and their interaction also on $rETR_{max}$, alpha and I_k (Table 2). $rETR_{max}$ followed the same pattern as described for growth rate in the previous section. At 51 Pa, $rETR_{max}$ of *G. oceanica* increased with increasing light radiation until 800 μmol photons m^{-2} s^{-1}. At higher P_{CO_2} levels, however, $rETR_{max}$ increased only until 400 μmol photons m^{-2} s^{-1} or 600 μmol photons m^{-2} s^{-1} and decreased significantly thereafter (Fig. 2A; Table 3). At 50 μmol photons m^{-2} s^{-1}, 100 μmol photons m^{-2} s^{-1}, and 200 μmol photons m^{-2} s^{-1}, $rETR_{max}$ did not show any significant differences among the three P_{CO_2} treatments (Tukey Post hoc, all df = 2, all $p > 0.05$).

Increasing light intensity resulted in a relatively constant decrease in alpha (Fig. 2B). The decline of alpha from lowest to highest light intensities was 23%, 32%, and 57% for 51 Pa, 105 Pa, and 152 Pa, respectively (Tukey Post hoc, all df = 1, all $p < 0.001$) (Fig. 2B). At 50 μmol photons m^{-2} s^{-1} or 100 μmol photons m^{-2} s^{-1}, alpha was not significantly different among the three P_{CO_2} treatments (Tukey Post hoc, both df = 2, both $p > 0.05$). At 200 μmol photons m^{-2} s^{-1} or 400 μmol photons m^{-2} s^{-1}, alpha at 105 Pa P_{CO_2} was lower than at 51 and 152 Pa P_{CO_2} (Tukey Post hoc, both $p < 0.01$). At 800 μmol photons m^{-2} s^{-1}, alpha decreased significantly with elevated P_{CO_2} treatments (Tukey Post hoc, both $p < 0.01$). It seems that effects of P_{CO_2} levels on alpha were amplified by increasing light intensity (Fig. 2B).

Saturation light intensity, I_k, more than doubled from lowest to highest light intensities. With light intensity increasing from 50 μmol photons m^{-2} s^{-1} to 800 μmol photons m^{-2} s^{-1}, I_k increased about 2.2, 2.4, and 3.5 times for 51 Pa, 105 Pa, and 152 Pa, respectively (Tukey Post hoc, df = 1, $p < 0.001$) (Fig. 2C; Table 3). At 50 μmol photons m^{-2} s^{-1}, 100 μmol photons m^{-2} s^{-1}, or 200 μmol photons m^{-2} s^{-1}, I_k did not show significant difference among the three P_{CO_2} treatments (Tukey Post hoc, all df = 2, all $p > 0.1$). At 400 μmol photons m^{-2} s^{-1} or 600 μmol photons m^{-2} s^{-1}, I_k at 51 Pa P_{CO_2} was lower than at 105 and 152 Pa P_{CO_2} treatments (Tukey Post hoc, both df = 1, both $p < 0.05$). At 800 μmol photons m^{-2} s^{-1}, I_k increased significantly with elevated P_{CO_2} (Tukey Post hoc, df = 2, $p < 0.01$). It seems that the positive effect of P_{CO_2} treatment on I_k was also amplified by increasing light intensity (Fig. 2C).

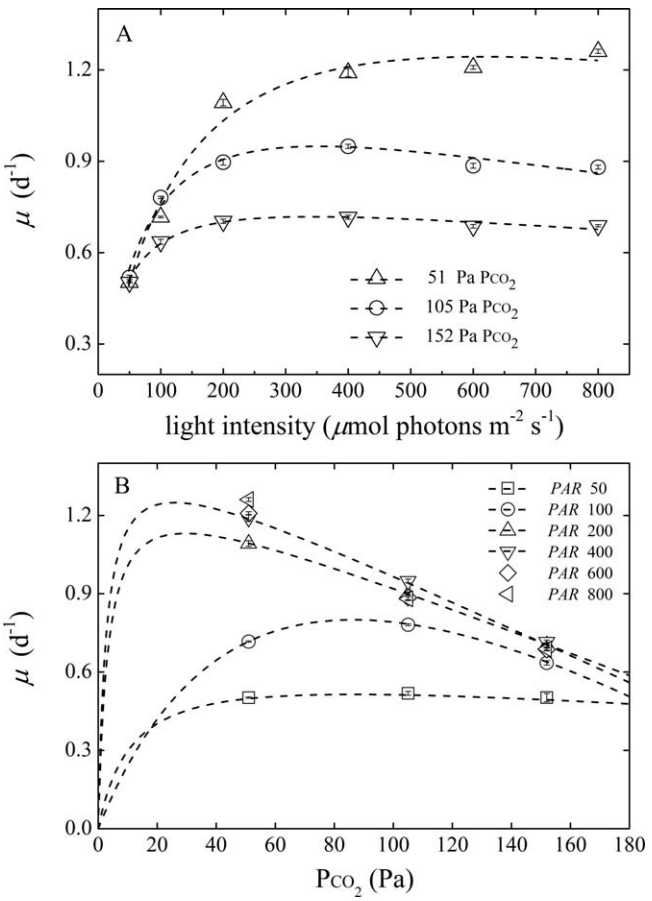

Fig. 1. Effects of light intensity and P_{CO_2} level on growth rate of *Gephyrocapsa oceanica*. (**A**) Growth rate as a function of light intensities at 51 (△), 105 (○) and 152 (▽) Pa P_{CO_2}. (**B**) Growth rate as a function of P_{CO_2} levels at light intensities of 50 μmol photons m^{-2} s^{-1}, 100 μmol photons m^{-2} s^{-1}, 200 μmol photons m^{-2} s^{-1}, 400 μmol photons m^{-2} s^{-1}, 600 μmol photons m^{-2} s^{-1} and 800 μmol photons m^{-2} s^{-1}. Dashed lines in panel (**A**) were fitted using Eq. 2. Dashed lines in panel (**B**) were fitted using Eq. 8. The values represent the mean of four replicates, with error bars showing ± one standard deviation. Please note that based on only three points, growth rate response curves at 600 μmol photons m^{-2} s^{-1} and 800 μmol photons m^{-2} s^{-1} in panel (**B**) cannot be fitted using Eq. 8.

Table 3. Experimental condition, growth rate, photosynthesis parameter and carbon production in dilute batch culture incubation.

P_{CO_2}	PAR	μ	$rETR_{max}$	alpha	I_k	POC/cell/d	PIC/cell/d	PIC/POC	POC/PON
51	50	0.50 (0.002)	95 (2)	0.29 (0.003)	321 (5)	8.18 (0.229)	10.79 (0.437)	1.30 (0.053)	7.55 (0.209)
	100	0.72 (0.003)	111 (3)	0.29 (0.001)	381 (11)	17.04 (0.670)	23.80 (2.492)	1.40 (0.146)	8.04 (0.316)
	200	1.09 (0.011)	117 (2)	0.27 (0.002)	434 (6)	19.51 (0.343)	33.80 (1.672)	1.73 (0.086)	6.74 (0.118)
	400	1.19 (0.013)	143 (2)	0.26 (0.004)	539 (4)	33.85 (2.514)	46.58 (12.711)	1.38 (0.097)	7.22 (0.536)
	600	1.21 (0.006)	154 (3)	0.23 (0.006)	678 (14)	32.59 (1.028)	52.69 (4.065)	1.62 (0.125)	7.32 (0.231)
	800	1.26 (0.007)	157 (2)	0.23 (0.006)	692 (10)	29.47 (0.233)	48.78 (1.374)	1.66 (0.047)	6.90 (0.055)
105	50	0.52 (0.007)	92 (1)	0.29 (0.002)	316 (5)	7.07 (0.098)	6.96 (0.311)	0.98 (0.439)	6.75 (0.094)
	100	0.78 (0.004)	101 (2)	0.29 (0.002)	352 (6)	17.84 (0.722)	17.27 (1.472)	0.97 (0.825)	6.73 (0.273)
	200	0.90 (0.010)	126 (2)	0.26 (0.004)	487 (8)	25.82 (3.484)	19.19 (3.577)	0.74 (0.139)	6.91 (0.933)
	400	0.95 (0.007)	157 (3)	0.24 (0.003)	643 (9)	28.66 (4.087)	18.71 (4.367)	0.65 (0.152)	6.05 (0.863)
	600	0.89 (0.008)	180 (10)	0.24 (0.005)	748 (38)	21.16 (1.988)	23.35 (2.075)	1.10 (0.098)	5.99 (0.563)
	800	0.88 (0.007)	155 (17)	0.20 (0.010)	773 (71)	19.89 (1.391)	21.64 (0.777)	1.12 (0.040)	6.27 (0.451)
152	50	0.50 (0.016)	84 (4)	0.28 (0.003)	295 (11)	8.19 (0.077)	5.55 (2.157)	0.81 (0.013)	6.76 (0.052)
	100	0.64 (0.008)	112 (2)	0.29 (0.004)	381 (4)	12.53 (1.106)	7.03 (1.457)	0.56 (0.116)	6.81 (0.601)
	200	0.70 (0.007)	130 (3)	0.27 (0.002)	471 (13)	15.52 (2.054)	8.13 (2.252)	0.52 (0.145)	7.62 (1.008)
	400	0.72 (0.006)	171 (10)	0.26 (0.006)	654 (35)	12.96 (0.938)	14.01 (1.585)	1.08 (0.122)	6.83 (0.494)
	600	0.69 (0.006)	153 (7)	0.20 (0.006)	773 (39)	13.88 (1.468)	10.33 (1.083)	0.74 (0.078)	6.50 (0.687)
	800	0.69 (0.004)	130 (11)	0.12 (0.011)	1028 (20)	14.92 (2.454)	13.26 (0.748)	0.89 (0.050)	6.20 (1.020)

POC/cell/d, particulate organic carbon production rate (pg C $cell^{-1}$ d^{-1}); PIC/cell/d, particulate inorganic carbon production rate (pg C $cell^{-1}$ d^{-1}); PIC/POC, PIC : POC ratio; POC/PON, POC : PON ratio. More detailed information is given as in Table 2. The values are expressed as the mean of four replicates. Data in the brackets are the standard deviations for four replicates.

POC production rate

Both, changing carbonate chemistry conditions and light intensity independently and interactively affected POC production rates (Table 2). POC production rates increased significantly at 51 Pa and 105 Pa with increasing light intensity until 400 μmol photons m^{-2} s^{-1}. At 51 Pa, POC production rates did not show a significant difference at 400–800 μmol photons m^{-2} s^{-1} (Tukey Post hoc, df = 1, $p > 0.1$) (Fig. 3A). At 105 Pa, POC production rates decreased significantly when light intensity increased from 400 μmol photons m^{-2} s^{-1} to 800 μmol photons m^{-2} s^{-1} (Tukey Post hoc, df = 1, $p < 0.001$) (Fig. 3A; Table 3). In comparison to 51 Pa, measured POC production rates at 105 Pa P_{CO_2} were higher at 200 μmol photons m^{-2} s^{-1} (Tukey Post hoc, df = 1, $p < 0.01$), but significantly lower at 400 μmol photons m^{-2} s^{-1}, 600 μmol photons m^{-2} s^{-1}, and 800 μmol photons m^{-2} s^{-1} (Fig. 3A,B).

Table 4. Calculated maximum values for growth, POC and PIC production rates. At each P_{CO_2} level, growth, POC and PIC production rates were fitted using equation 2, and the maximum values were calculated according to equation 4.

P_{CO_2} (Pa)	Maximum growth rate (d^{-1})	Maximum POC production rate (pg C $cell^{-1}$ d^{-1})	Maximum PIC production rate (pg C $cell^{-1}$ d^{-1})
51	1.24 ± 0.01^a	34.42 ± 2.65^a	49.90 ± 2.59^a
105	0.95 ± 0.01^b	29.33 ± 4.30^a	22.44 ± 1.44^b
152	0.72 ± 0.01^c	14.72 ± 0.94^b	12.78 ± 0.64^c

Different letters represent statistical different means (Tukey Post hoc, $p < 0.001$). The values are expressed as the mean of four replicates ± one standard deviation.

At 152 Pa, POC production rates increased with enhanced light radiation until 200 μmol photons m^{-2} s^{-1} (Tukey Post hoc, df = 1, $p < 0.05$) and levelled off with further increases in light intensity (Tukey Post hoc, df = 3, $p > 0.05$) (Fig. 3A). At 50 μmol photons m^{-2} s^{-1}, POC production rates did not show any difference at the three P_{CO_2} treatments (Tukey Post hoc, all df = 2, $p > 0.1$) (Fig. 3A,B). At 100–800 μmol photons m^{-2} s^{-1}, POC production rates at high P_{CO_2} were lower than at intermediate P_{CO_2} (Tukey Post hoc, all df = 1, $p < 0.05$ at 100, 200, 400, and 600 treatments; $p > 0.05$ at 800 treatment). At 400 μmol photons m^{-2} s^{-1}, 600 μmol photons m^{-2} s^{-1}, and 800 μmol photons m^{-2} s^{-1}, POC production rates at intermediate P_{CO_2} were significantly lower than at low P_{CO_2} (Tukey Post hoc, all df = 1, $p < 0.05$). Maximum POC production rates at 51 and 105 Pa P_{CO_2} were not significantly different (Tukey Post hoc, df = 1, both $p > 0.05$), and were higher than that at 152 Pa P_{CO_2} (Tukey Post hoc, df = 1, both $p < 0.001$) (Table 4).

PIC production rate

Both, changing carbonate chemistry conditions and light intensity independently and interactively affected PIC production rates (Table 2). At 50 μmol photons m^{-2} s^{-1}, PIC production rates decreased by about 35% and 48% from low to intermediate and high P_{CO_2} (Tukey Post hoc, both df = 1,

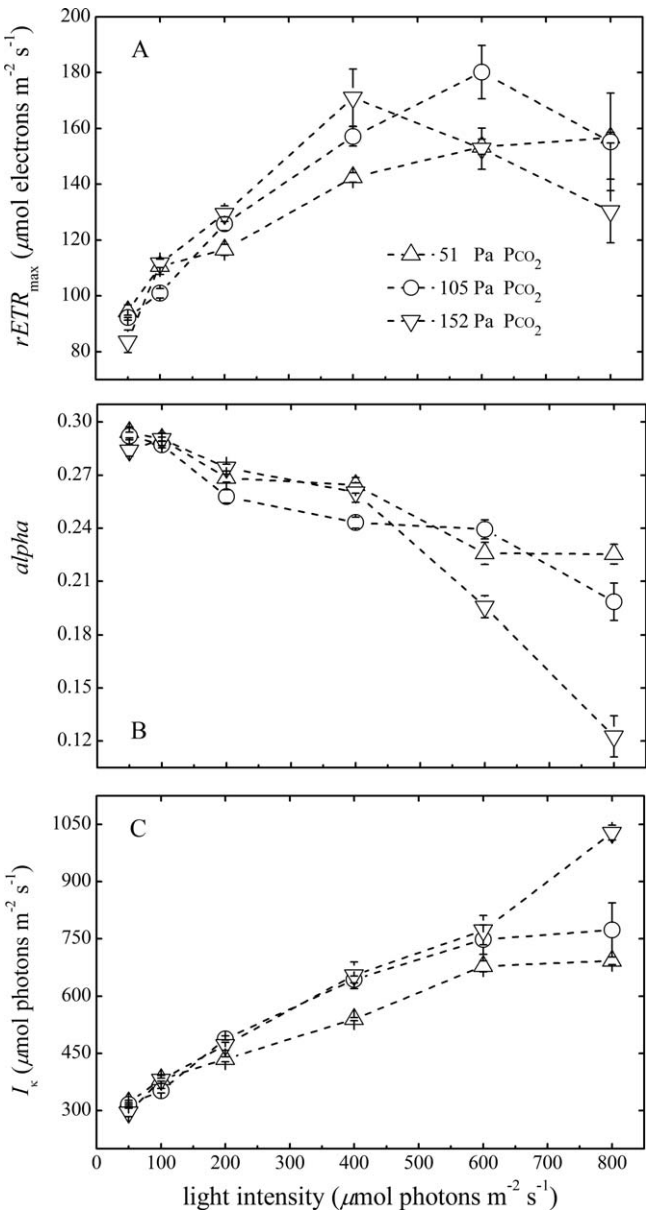

Fig. 2. $rETR_{max}$, alpha and I_k of *G. oceanica* as a function of light intensities at 51 (△), 105 (○) and 152 (▽) Pa P_{CO_2}. (**A**) The maximum of rETR ($rETR_{max}$) as a function of light intensity. (**B**) The initial slope of the light limited part of the P-I curve (alpha) as a function of light intensity. (**C**) Saturation light intensity (I_k) as a function of light intensity. $rETR_{max}$ was calculated according to Eq. 4, alpha was calculated with Eq. 3, and I_k was calculated from the expression $rETR_{max}$/alpha. The values represent the mean of four replicates, with error bars representing ± one standard deviation.

both $p > 0.05$) (Fig. 3C,D; Table 3). At 100–800 μmol photons m^{-2} s^{-1}, PIC production rates decreased by 27–56% at 105 Pa, and by 65–80% at 152 Pa in comparison to 51 Pa (Tukey Post hoc, all df = 1, all $p < 0.001$).

Light intensity had a positive effect on calcification rates at 51 and 105 Pa P_{CO_2} levels (Fig. 3C; Table 3). At 51 Pa P_{CO_2}, calcification rates were enhanced by about 4.5 times with enhanced light radiation until 800 μmol photons m^{-2} s^{-1}. At 105 Pa P_{CO_2}, PIC production rates only increased until 100 μmol photons m^{-2} s^{-1} but stayed constant with a further increase in light intensity (Tukey Post hoc, df = 4, all $p > 0.05$). At 152 Pa P_{CO_2}, PIC production rates did not show significant differences among six light treatments (Tukey Post hoc, df = 5, all $p > 0.05$). Maximum PIC production rates declined significantly with rising P_{CO_2} levels (one-way ANOVA, $F = 484$, df = 2, $p < 0.001$; Tukey Post hoc, df = 2, $p < 0.001$) (Table 4).

PIC : POC ratio and POC : PON ratio

Both, changing carbonate chemistry conditions and light intensity independently and interactively affected PIC : POC ratio and POC : PON ratio (Table 2). At each light treatment, PIC : POC ratios at 51 Pa P_{CO_2} were significantly higher than at 105 and 152 Pa P_{CO_2} (Tukey Post hoc, df = 1, $p < 0.05$) (Fig. 3E). Significant differences in PIC : POC ratios between 105 Pa and 152 Pa P_{CO_2} were found at 100 μmol photons m^{-2} s^{-1}, 400 μmol photons m^{-2} s^{-1}, and 600 μmol photons m^{-2} s^{-1} (Tukey Post hoc, all df = 1, all $p < 0.01$). There was no obvious trend between PIC : POC ratio and light intensity.

Both, elevated P_{CO_2} and higher light intensity reduced POC : PON ratios (Tukey Post hoc, df = 1, $p > 0.05$) (Fig. 3F). At 51 Pa P_{CO_2}, POC : PON ratios at 50 μmol photons m^{-2} s^{-1} and 100 μmol photons m^{-2} s^{-1} were slightly higher than at other treatment conditions (Tukey Post hoc, all $p > 0.05$) (Table 3).

Discussion

Changing carbonate chemistry modulates the light responses of photosynthetic carbon fixation, calcification and growth rates

POC production and growth rates of marine phytoplankton usually increase with increasing light intensity, level off at saturating light intensities and then decline again at inhibiting light levels (e.g., Geider et al. 1997; Gao et al. 2012; Fig. 4A). By fitting the light response curve given in Eq. 2 to our data, we found that rising P_{CO_2} reduced the maximum rates of growth and photosynthetic carbon fixation (Figs. 1A, 3A; Table 4). Presumably, rising P_{CO_2} could reduce the need for CCM activity thereby saving energy (Raven 1991; Hopkinson et al. 2011; McCarthy et al. 2012). In our case, the lower potential for energy dissipation toward higher P_{CO_2} (lower CCM activity) may exacerbate photo inhibition thereby explaining the reduced growth and POC production rates (Figs. 1, 3).

Another reason for higher growth and POC production rates at lower P_{CO_2} and increasing light intensities (Figs. 1B, 3B) may be that increasing light intensities facilitate the operation of CCMs (Rokitta and Rost 2012) thereby enabling cells to satisfy their inorganic carbon requirements for POC

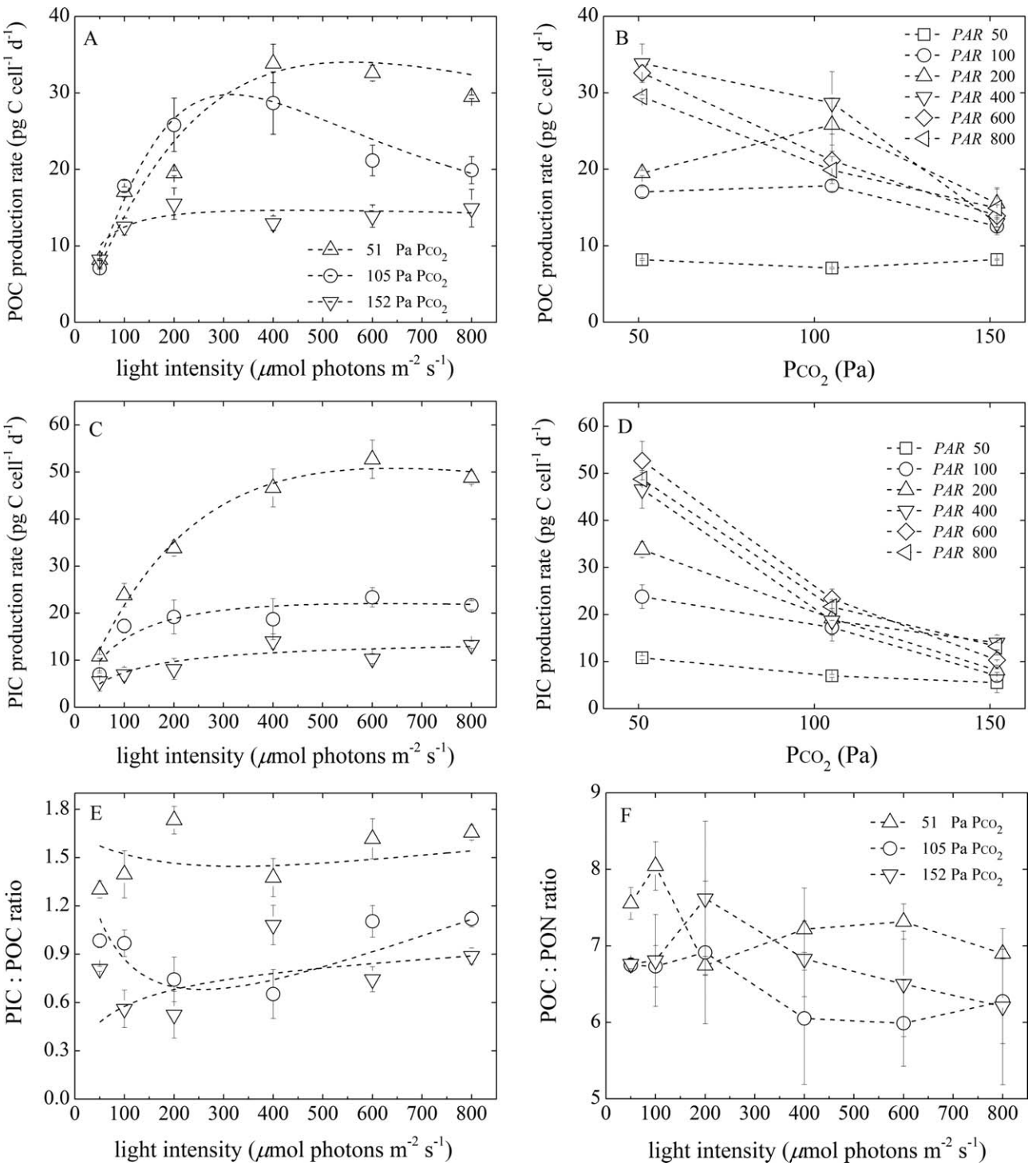

Fig. 3. Effects of light intensity and P_{CO_2} level on POC and PIC production rates, PIC : POC ratio and POC : PON ratio of *G. oceanica*. Panels (**A**), (**C**), (**E**), (**F**) depict POC production rate, PIC production rate, PIC : POC ratio and POC : PON ratio as a function of light intensities at 51 (△), 105 (○) and 152 (▽) Pa P_{CO_2}. Panels (**B**), (**D**) show POC production rate and PIC production rate as a function of P_{CO_2} at 50 μmol photons m^{-2} s^{-1}, 100 μmol photons m^{-2} s^{-1}, 200 μmol photons m^{-2} s^{-1}, 400 μmol photons m^{-2} s^{-1}, 600 μmol photons m^{-2} s^{-1}, and 800 μmol photons m^{-2} s^{-1}. The values represent the mean of four replicates, with error bars representing ± one standard deviation.

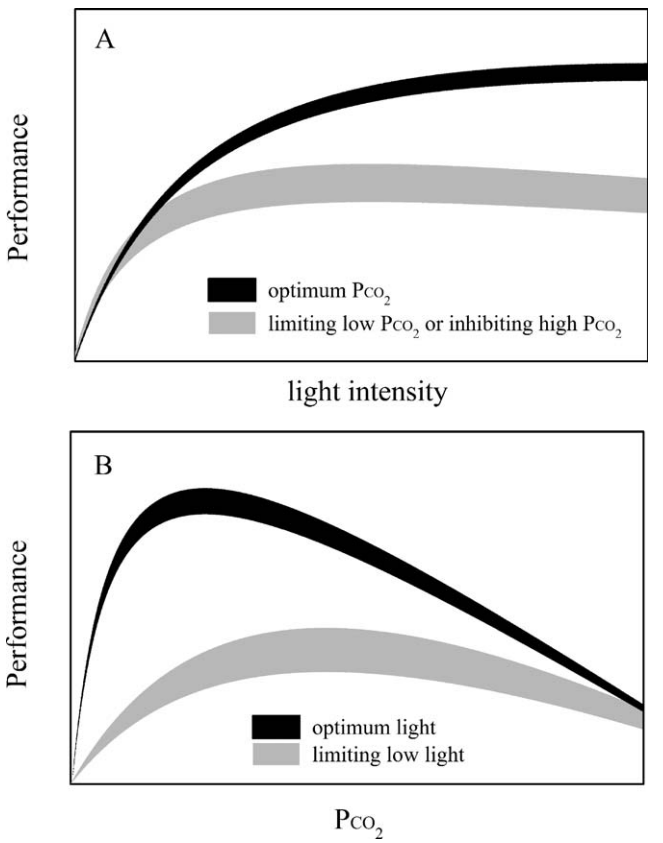

Fig. 4. Conceptual drawing for the interactive effects of light intensity and P_{CO_2} level on the performance (representing growth, photosynthetic carbon fixation, and calcification) of *G. oceanica*. (**A**) The modulating effect of P_{CO_2} on the light response curve. Maximum rates at limiting low P_{CO_2} and inhibiting high P_{CO_2} are lower than at optimum P_{CO_2}. (**B**) The modulating effect of light intensity on the P_{CO_2} sensitivity. Limiting low light intensity shifts the P_{CO_2} optimum toward higher level and reduces the maximum rate.

production and growth rates already at lower P_{CO_2} levels. In fact, at high light intensity, high P_{CO_2} grown cells were found to possess less photosystem I (PS1) per cell and keep a smaller proportion of PSII complexes open compared with low P_{CO_2} grown cells (Burns et al. 2006). Lower PSI and PSII absorbance capacities for light in high P_{CO_2} grown cells could also be expected to lead to lower POC production and growth rates. Furthermore, the proton concentration ($[H^+]$) in the cytosol of the coccolithophore *Emiliania huxleyi* was found to increase with increasing $[H^+]$ in seawater (Suffrian et al. 2011). Cells growing at high P_{CO_2} could suffer from the negative effect of high $[H^+]$ on POC production (Bach et al. 2011) even more so as this effect may be exacerbated by high light intensities (Ihnken et al. 2011).

Calcification is an energy-dependent process and often reduced in coccolithophores at P_{CO_2} levels projected for the end of this century (Riebesell and Tortell 2011; Meyer and Riebesell 2015). However, only some studies focussed on the interactive effects of CO_2 concentration and light intensity on coccolithophore calcification (Zondervan et al. 2002; Feng et al. 2008; Gao et al. 2009; Rokitta and Rost 2012). In this study, a increasing light intensity accelerated calcification rates strongly at lower P_{CO_2} whereas this positive effect was absent at higher P_{CO_2} (Fig. 3C), similar to growth and photosynthetic carbon fixation rates. This supports earlier findings that the sensitivity of calcification rates to light intensity can be modulated by carbonate chemistry (Zondervan et al. 2002; Feng et al. 2008; Gao et al. 2009; Rokitta and Rost 2012). The underlying physiological explanation could be that at limiting light intensity, light is the dominant factor determining the calcification rate and differences in carbonate chemistry conditions are presumably less important. This can be seen at the lowest light intensity in this study (50 μmol photons m^{-2} s^{-1}), where PIC production rates did not show a significant difference among the three P_{CO_2} treatments (Fig. 3D). At saturating light intensity, however, differences in CO_2 or H^+ apparently induce a significant effect on calcification rates (Feng et al. 2008).

For P_{CO_2} levels lower than 29 Pa, Sett et al. (2014) concluded that POC and PIC production and growth rates in the same *G. oceanica* strain were limited by inorganic carbon availability. Although such low P_{CO_2} levels were not included in our study, by fitting the light response curves (Figs. 1A, 3A,C) we conclude that both limiting low P_{CO_2} and inhibiting high P_{CO_2} levels reduce the maximum values for photosynthetic carbon fixation, calcification and growth rates of coccolithophores (Fig. 4A; Table 4).

Rising P_{CO_2} and increasing light intensity synergistically alter the electron transport rate in the light reaction

rETR is a measure for photosynthetic efficiency (Schreiber et al. 1995). To acclimate to high irradiances, phytoplankton cells regulate the photosystem stoichiometry (PSI : PSII) by lowering the amount of photosystem I (PSI) reaction centers relative to PSII complexes (Sonoike et al. 2001). Here we found that the $rETR_{max}$ response of *G. oceanica* (Fig. 2A) to high light intensities was depending on the incubation P_{CO_2} which implies that different P_{CO_2} levels induced changes in PSI : PSII. A study by Burns et al. (2006) revealed that at high light intensity, low P_{CO_2} grown cells contained significantly more PsaC protein (core subunit of photosystem I) in the PSI complex than high P_{CO_2} grown cells. Furthermore, Burns et al. (2006) found that across the range of growth irradiances, PsaC : PSII absorbance capacity (an indicator of PSI content relative to the capacity of PSII to capture light energy) increased in low P_{CO_2} grown cells, whereas they slightly decreased in high P_{CO_2} grown cells. Thus, the observed reduction in $rETR_{max}$ with increasing P_{CO_2} at high light intensities may be due to lower PSI : PSII.

Phytoplankton can alter light absorption for photosynthesis to enable acclimation over a wide range of irradiances (Henriksen et al. 2002). Algae tend to reduce the

pigment contents such as chlorophyll *a*, carotenoids or fucoxanthin in antenna systems to prevent excessive energy to be transferred to PSII reaction centres (Henriksen et al. 2002; Barcelos e Ramos et al. 2012). At 50 μmol photons m^{-2} s^{-1} in this study, the quantum yield of PSII (F_v/F_m, the ratio of photons transferred in the ETR to photons absorbed by PSII) at 152 Pa was only 6% lower than at 51 Pa. However, at 800 μmol photons m^{-2} s^{-1} the quantum yield of PSII at 152 Pa was 30% lower than at 51 Pa (data not shown). This indicates that high light intensity and high P_{CO_2} may synergistically reduce the quantum yield of PSII (the maximum efficiency of PSII), which leads to large diminution in alpha at high P_{CO_2} and high light conditions (Fig. 2B).

Light intensity modulates the P_{CO_2} sensitivity of photosynthetic carbon fixation, calcification and growth rates

Physiological responses to a broad range of P_{CO_2} levels of coccolithophores investigated in this respect so far displayed optimum curve patterns (Langer et al. 2006; Bach et al. 2011, 2015; Sett et al. 2014; Müller et al. 2015). Growth and production rates of POC and PIC increase with increasing P_{CO_2} levels, reach a maximum, and then decline linearly with further P_{CO_2} (proton concentration ($[H^+]$)) increase (Bach et al. 2011; Sett et al. 2014; Bach et al. 2015; Fig. 4B). The CO_2 and HCO_3^- availability was identified as the factor responsible for the observed decline of growth and production rates toward the left side of the optimum, the proton concentration ($[H^+]$) was the driving factor toward the right side of the optimum (Bach et al. 2011, 2015). The sensitivities of these rates to inorganic carbon availability and H^+ were clearly modulated by light intensity (Figs. 1B, 3B,D). Light availability is likely to affect the supply of inorganic carbon to photosynthesis, calcification and growth in general (Zondervan et al. 2002; Barcelos e Ramos et al. 2012; Rokitta and Rost 2012).

We did not directly determine the P_{CO_2} optimum for PIC production rates in this study as our treatment levels were limited. Sett et al. (2014), however, found that the P_{CO_2} optimum for calcification in the same *G. oceanica* strain was at about 29 Pa at 20°C and 150 μmol photons m^{-2} s^{-1}. According to this, the lowest P_{CO_2} level applied in our study (51 Pa) was too high to detect the optimum of the *G. oceanica* P_{CO_2} response curve. Nevertheless, assuming an optimum curve response and using the model described in Bach et al. (2011) as given in Eq. 8, the optimum P_{CO_2} for photosynthetic carbon fixation, calcification and growth rates shift toward lower levels with increasing light intensities (Figs. 1B, 3B). This is in line with findings by Rokitta and Rost (2012) who showed that the half-saturation DIC concentrations for carbon fixation of the calcifying algae *E. huxleyi* were 111 μmol kg^{-1} at 50 μmol photons m^{-2} s^{-1} and 20 μmol kg^{-1} at 300 μmol photons m^{-2} s^{-1}. The reasons for the shift could be

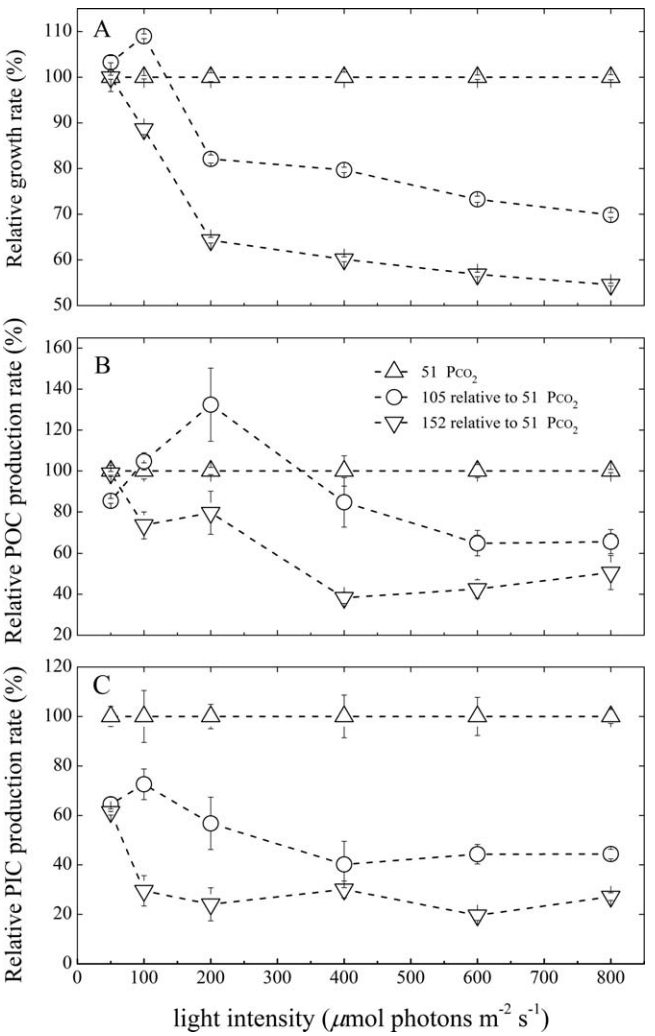

Fig. 5. Comparison of growth, POC and PIC production rates at 105 (○) and 152 (▽) Pa P_{CO_2} relative to those at 51 (△) Pa P_{CO_2}. The values represent the mean of four replicates, with error bars representing ± one standard deviation.

that higher light intensities provide more energy to allow for higher CCM activity which would help to overcome carbon limitation at lower P_{CO_2} levels (McGinn et al. 2003; Rokitta and Rost 2012). Following the growth rate response to light intensity shown in Fig. 1A, growth rate is expected to decrease toward increasingly inhibiting high light intensities beyond the measurement range of 800 μmol photons m^{-2} s^{-1}. If growth rates would drop more pronounced at low than at high P_{CO_2} levels, the P_{CO_2} optimum for growth shown in Fig. 1B is expected to be higher at inhibiting high light than at optimum light intensity.

Based on the results of this and other studies (Zondervan et al. 2002; Rost et al. 2003), we conclude that the optimum P_{CO_2} levels for growth, POC and PIC production rates at limiting low light are higher than at optimum light intensities (Figs. 1B, 3B,D, 4B). Furthermore, the maximum values for

these rates are lower at limiting low light than at optimum light intensities (Fig. 4B).

In an earlier study with *E. huxleyi*, Rokitta and Rost (2012) put forward a light dependent model suggesting that the rate of a physiological process is governed primarily by light intensity, and changes in P_{CO_2} levels will exacerbate or weaken the effects of light intensity on this rate. Our data supported the light dependent model (Figs. 1, 3). However, Rokitta and Rost (2012) found that the sensitivities of POC and PIC production rates of *E. huxleyi* to high P_{CO_2} are stronger at 50 μmol photons m^{-2} s^{-1} than at 300 μmol photons m^{-2} s^{-1}, whereas we observed a stronger effect of high P_{CO_2} on POC and PIC production rates at 600–800 μmol photons m^{-2} s^{-1} compared with 50 μmol photons m^{-2} s^{-1} (Fig. 5). This discrepancy is possibly due to the variable sensitivities of *E. huxleyi* and *G. oceanica* to light and P_{CO_2}.

The results of our study show that increasing light intensity decreases the P_{CO_2} optima for carbon fixation, calcification and growth rates of *G. oceanica*. In contrast, rising temperature had the opposite effect, increasing the P_{CO_2} optima for these rates (Sett et al. 2014). These opposing trends are likely due to the fact that temperature primarily modulates carbon demand by accelerating metabolic activity, whereas light also affects carbon supply through energy provision to carbon uptake mechanisms. In the future ocean, both light intensity and temperature in the upper mixed layer will generally increase (Sarmiento et al. 2004; IPCC 2013). How these combined effects will affect the competitive fitness of this and other coccolithophore species under future ocean scenarios is difficult to predict with the information presently available (Riebesell and Gattuso 2015). It emphasizes the need for further investigation on the interacting effect of simultaneous modification of life-sustaining properties such as temperature, CO_2, light, and nutrients in the marine environment.

References

Bach, L. T., U. Riebesell, and K. G. Schulz. 2011. Distinguishing between the effects of ocean acidification and ocean carbonation in the coccolithophore *Emiliania huxleyi*. Limnol. Oceanogr. **56**: 2040–2050. doi:10.4319/lo.2011.56.6.2040

Bach, L. T., U. Riebesell, M. A. Gutowska, L. Federwisch, and K. G. Schulz. 2015. A unifying concept of coccolithophore sensitivity to changing carbonate chemistry embedded in an ecological framework. Prog. Oceanogr. **135**: 125–138. doi:10.1016/j.pocean.2015.04.012

Barcelos e Ramos, J., K. G. Schulz, S. Febiri, and U. Riebesell. 2012. Photoacclimation to abrupt changes in light intensity by *Phaeodactylum tricornutum* and *Emiliania huxleyi*: The role of calcification. Mar. Ecol. Prog. Ser. **452**: 11–26. doi:10.3354/meps09606

Björkman, O., and B. Demmig. 1987. Photon yield of O_2 evolution and chlorophyll fluorescence characteristics at 77 K among vascular plants of diverse origins. Planta **170**: 489–504. doi:10.1007/BF00402983

Bopp, L., and others. 2001. Potential impact of climate change on marine export production. Global Biogeochem. Cycles **15**: 81–99. doi:10.1029/1999GB001256

Braarud, T., K. R. Gaarder, J. Marklaki, and E. Nordli. 1952. Coccolithophorids studied in the electron microscope. Observations on *Coccolithus huxleyi* and *Syracosphaera carterae*. Nytt Mag. Bot. **1**: 129–134.

Burns, R. A., T. D. B. MacKenzie, and D. A. Campbell. 2006. Inorganic carbon repletion constrains steady-states light acclimation in the cyanobacterium *Synechococcus elongatus*. J. Phycol. **42**: 610–621. doi:10.1111/j.1529-8817.2006.00220.x

Danbara, A., and Y. Shiraiwa. 1999. The requirement for selenium for the growth of marine coccolithophorids, *Emiliania huxleyi*, *Gephyrocapsa oceanica* and *Helladosphaera* sp. (Prymnewsiophyceae). Plant Cell Physiol. **40**: 762–766. doi:10.1093/oxfordjournals.pcp.a029603

Dickson, A. G., J. D. Afghan, and G. C. Anderson. 2003. Reference materials for oceanic CO_2 analysis: A method for the certification of total alkalinity. Mar. Chem. **80**: 185–197. doi:10.1016/S0304-4203(02)00133-0

Eilers, P., and J. Peeters. 1988. A model for the relationship between light intensity and the rate of photosynthesis in phytoplankton. Ecol. Model. **42**: 199–215. doi:10.1016/0304-3800(88)90057-9

Feng, Y., M. E. Warner, Y. Zhang, J. Sun, F. X. Fu, J. M. Rose, and D. A. Hutchins. 2008. Interactive effects of increased P_{CO_2}, temperature and irradiance on the marine coccolithophore *Emiliania huxleyi* (Prymnesiophyceae). Eur. J. Phycol. **43**: 87–98. doi:10.1080/09670260701664674

Gao, K., Z. Ruan, V. E. Villafañe, J. P. Gattuso, and E. W. Helbling. 2009. Ocean acidification exacerbates the effect of UV radiation on the calcifying phytoplankton *Emiliania huxleyi*. Limnol. Oceanogr. **54**: 1855–1862. doi:10.4319/lo.2009.54.6.1855

Gao, K., and others. 2012. Rising CO_2 and increased light exposure synergistically reduce marine primary productivity. Nat. Clim. Change **2**: 519–523. doi:10.1038/nclimate1507

Geider, R. J., H. L. MacIntyre, and T. M. Kana. 1997. Dynamic model of phytoplankton growth and acclimation: Responses of the balanced growth rate and the chlorophyll a: carbon ratio to light, nutrient-limitation and temperature. Mar. Ecol. Prog. Ser. **148**: 187–200. doi:10.3354/meps148187

Giordano, M., J. Beardall, and J. A. Raven. 2005. CO_2 concentrating mechanisms in algae: Mechanisms, environmental modulation and evolution. Annu. Rev. Plant Biol. **56**: 99–131. doi:10.1146/annurev.arplant.56.032604.144052

Guillard, R. R., and J. H. Ryther. 1962. Studies of marine planktonic diatoms. I. *Cyclotella nana* Hustedt, and *Detonula confervacea* (cleve) Gran. Can. J. Microbiol. **8**: 229–239. doi:10.1139/m62-029

Henriksen, P., B. Riemann, H. Kaas, H. M. Sørensen, and H. L. Sørensen. 2002. Effects of nutrient-limitation and

irradiance on marine phytoplankton pigments. J. Plankton Res. **24**: 835–858. doi:10.1093/plankt/24.9.835

Hopkinson, B. M., C. L. Dupont, A. E. Allen, and F. M. M. Morel. 2011. Efficiency of the CO_2-concentrating mechanism of diatoms. Proc. Natl. Acad. Sci. USA **8**: 3830–3837. doi:10.1073/pnas.1018062108

Houghton, J. T., and others. 2001. Climate change 2001: The scientific basis, p. 36–40. Cambridge Univ. Press.

Ihnken, S., S. Roberts, and J. Beardall. 2011. Differential responses of growth and photosynthesis in the marine diatom *Chaetoceros muelleri* to CO_2 and light availability. Phycologia **50**: 182–193. doi:10.2216/10-11.1

Intergovernmental Panel on Climate Change (IPCC). 2013. Summary for Policymakers, p: 3–33. *In* T. F. Stocker, and others [eds.], Climate change 2013: The physical science basis. Contribution of Working Group I to the Fifth Assessment Report of the Intergovernmental Panel on Climate Change. Cambridge Univ. Press.

Kaeriyama, H., F. Katsuki, M. Otsubo, M. Yamada, K. Ichimi, K. Tada, and P. J. Harrison. 2011. Effects of temperature and irradiance on growth of strains belonging to seven *Skeletonema* species isolated from Dokai Bay, southern Japan. Eur. J. Phycol. **46**: 113–124. doi:10.1080/09670262.2011.565128

Kester, D., I. W. Duedall, D. N. Connors, and R. M. Pytkowicz. 1967. Preparation of artificial seawater. Limnol. Oceanogr. **1**: 176–179. doi:10.4319/lo.1967.12.1.0176

Langer, G., M. Geisen, K. H. Baumann, J. Kläs, U. Riebesell, S. Thoms, and J. R. Young. 2006. Species-specific responses of calcifying algae to changing seawater carbonate chemistry. Geochem. Geophys. Geosyst. **7**: 1–12. doi:10.1029/2005GC001227

McCarthy, A., S. P. Rogers, S. J. Duffy, and D. A. Campbell. 2012. Elevated carbon dioxide differentially alters the photophysiology of *Thalassiosira pseudonana* (Bacillariophyceae) and *Emiliania huxleyi* (Haptophyta). J. Phycol. **48**: 635–646. doi:10.1111/j.1529-8817.2012.01171.x

McGinn, P. J., G. D. Price, R. Maleszka, and M. R. Badger. 2003. Inorganic carbon limitation and light control the expression of transcripts related to the CO_2-concentrating mechanism in the cyanobacterium *Synechocystis* sp. strain PCC 6803. Plant Physiol. **132**: 218–229. doi:10.1104/pp.102.019349

Merico, A., T. Tyrrell, E. J. Lessard, T. Oguz, P. J. Stabeno, S. I. Zeeman, and T. E. Whitledge. 2004. Modelling phytoplankton succession on the Bering Sea shelf: Role of climate influences and trophic interactions in generating *Emiliania huxleyi* blooms 1997–2000. Deep-Sea Res. Part I **51**: 1803–1826. doi:10.1016/j.dsr.2004.07.003

Meyer, J., and U. Riebesell. 2015. Reviews and syntheses: Responses of coccolithophores to ocean acidification: A meta-analysis. Biogeosciences **12**: 1671–1682. doi:10.5194/bg-12-1671-2015

Müller, M. N., T. W. Trull, and G. M. Hallegraeff. 2015. Different responses of three Southern Ocean *Emiliania huxleyi* ecotypes to changing seawater carbonate chemistry. Mar. Ecol. Prog. Ser. **531**: 81–90. doi:10.3354/meps11309

Pierrot, D., E. Lewis, and D. W. R. Wallace. 2006. MS Excel program developed for CO_2 system calculations. ORNL/CDIAC-105. Carbon Dioxide Information Analysis Centre, Oak Ridge National Laboratory, U.S. Department of Energy. doi:10.3334/CDIAC/otg.CO2SYS_XLS_CDIAC105a

Raven, J. A. 1991. Physiology of inorganic C acquisition and implications for resource use efficiency by marine phytoplankton: Relation to increased CO_2 and temperature. Plant Cell Environ. **14**: 779–794. doi:10.1111/j.1365-3040.1991.tb01442.x

Riebesell, U. 2004. Effects of CO_2 enrichment on marine phytoplankton. J. Oceanogr. **60**: 719–729. doi:10.1007/s10872-004-5764-z

Riebesell, U., and P. D. Tortell. 2011. Effects of ocean acidification on pelagic organisms and ecosystems, p. 99–121. *In* J. P. Gattuso and L. Hansson [eds.], Ocean acidification. Oxford Univ. Press.

Riebesell, U., and J. P. Gattuso. 2015. Lessons learned from ocean acidification research. Nat. Clim. Chang. **5**: 12–14. doi:10.1038/nclimate2456

Rokitta, S. D., and B. Rost. 2012. Effects of CO_2 and their modulation by light in the life-cycle stages of the coccolithophore *Emiliania huxleyi*. Limnol. Oceanogr. **57**: 607–618. doi:10.4319/lo.2012.57.2.0607

Rost, B., U. Riebesell, and S. Burkhardt. 2003. Carbon acquisition of bloom-forming marine phytoplankton. Limnol. Oceanogr. **48**: 56–67. doi:10.4319/lo.2003.48.1.0055

Rost, B., and U. Riebesell. 2004. Coccolithophores and the biological pump: Responses to environmental changes, p. 99–125. *In* H. R. Thierstein and J. R. Young [eds.], Coccolithophores: From molecular biology to global impact. Springer.

Roy, R. N., and others. 1993. Thermodynamics of the dissociation of boric acid in seawater at S 5 35 from 0 degrees C to 55 degrees C. Mar. Chem. **44**: 243–248. doi:10.1016/0304-4203(93)90206-4

Sabine, C. L., and others. 2004. The oceanic sink for anthropogenic CO_2. Science **305**: 367–371. doi:10.1126/science.1097403

Sarmiento, J. L., and others. 2004. Response of ocean ecosystems to climate warming. Global Biogeochem. Cycle **18**: GB3003. doi:10.1029/2003GB002134

Schippers, P., M. Lürling, and M. Scheffer. 2004. Increase of atmospheric CO_2 promotes phytoplankton productivity. Ecol. Lett. **7**: 446–451. doi:10.1111/j.1461-0248.2004.00597.x

Schreiber, U., W. Bilger, and C. Neubauer. 1995. Chlorophyll fluorescence as a nonintrusive indicator for rapid assessment of in vivo photosynthesis, p. 49–70. *In* E. D. Schulze and M. M. Caldwell [eds.], Ecophysiology of photosynthesis. Springer.

Sett, S., L. T. Bach, K. G. Schulz, S. Koch-Klavsen, M. Lebrato, and U. Riebesell. 2014. Temperature modulates coccolithophorid sensitivity of growth, photosynthesis and calcification to increasing seawater P_{CO_2}. PLoS ONE **9**: e88308. doi:10.1371/journal.pone.0088308

Sonoike, K., Y. Hihara, and M. Ikeuchi. 2001. Physiological significance of the regulation of photosystem stoichiometry upon high light acclimation of *Synechocystis* sp. PCC 6803. Plant Cell Physiol. **42**: 379–384. doi:10.1093/pcp/pce046

Suffrian, K., K. G. Schulz, M. A. Gutowska, U. Riebesell, and M. Bleich. 2011. Cellular pH measurements in *Emiliania huxleyi* reveal pronounced membrane proton permeability. New Phytol. **190**: 595–608. doi:10.1111/j.1469-8137.2010.03633.x

Xu, K., and K. S. Gao. 2012. Reduced calcification decreases photoprotective capability in the coccolithophorid *Emiliania huxleyi*. Plant Cell Physiol. **53**: 1267–1274. doi:10.1093/pcp/pcs066

Zondervan, I., B. Rost, and U. Riebesell. 2002. Effect of CO_2 concentration on the PIC/POC ratio in the coccolithophore *Emiliania huxleyi* grown under light-limiting conditions and different day lengths. J. Exp. Mar. Biol. Ecol. **272**: 55–70. doi:10.1016/S0022-0981(02)00037-0

Acknowledgments

The authors are grateful to Silke Lischka for reading and revising the manuscript, to Andrea Ludwig and Jana Meyer for dissolved inorganic carbon measurements, and to Kerstin Nachtigall for particulate organic and inorganic carbon measurements. We also thank the China Scholarship Council (CSC) for its support of Yong Zhang. This work was supported by the German Federal Ministry of Education and Research (Bundesministerium für Bildung und Forschung) in the framework of the collaborative project Biological Impacts of Ocean Acidification (BIOACID). Kai G. Schulz is the recipient of an Australian Research Council Future Fellowship (FT120100384).

Submitted 25 February 2015
Revised 29 July 2015
Accepted 3 August 2015

Associate editor: Heidi Sosik